

Wasserstein-Wasserstein Auto-Encoders

Shunkang Zhang¹, Yuan Gao², Yuling Jiao^{*3}, Jin Liu⁴, Yang Wang¹ and Can Yang^{†1}

¹*School of Mathematics and Statistics, Xi'an Jiaotong University*

²*School of Statistics and Mathematics, Zhongnan University of Economics and Law*

³*Department of Mathematics, The Hong Kong University of Science and Technology*

⁴*Center of Quantitative Medicine Duke-NUS Medical School*

Feb 24, 2019

Abstract

To address the challenges in learning deep generative models (e.g., the blurriness of variational auto-encoder and the instability of training generative adversarial networks), we propose a novel deep generative model, named Wasserstein-Wasserstein auto-encoders (WWAE). We formulate WWAE as minimization of the penalized optimal transport between the target distribution and the generated distribution. By noticing that both the prior P_Z and the aggregated posterior Q_Z of the latent code Z can be well captured by Gaussians, the proposed WWAE utilizes the closed-form of the squared Wasserstein-2 distance for two Gaussians in the optimization process. As a result, WWAE does not suffer from the sampling burden and it is computationally efficient by leveraging the reparameterization trick. Numerical results evaluated on multiple benchmark datasets including MNIST, fashion- MNIST and CelebA show that WWAE learns better latent structures than VAEs and generates samples of better visual quality and higher FID scores than VAEs and GANs.

1 Introduction

1.1 Literature review

Deep generative models (DGM) have proved powerful for extracting high-level representations from real-world data such as images, audios and texts. Benefiting from probabilistic

*Yuling Jiao (yulingjiaomath@whu.edu.cn)

†Can Yang (macyang@ust.hk)

formulations and neural network architectures, DGMs allow fast sampling and play a central role in many applications, such as text to image synthesis [25], style transfer [34], speech enhancement [24], text to speech synthesis [30]. Modern DGMs focus on mapping latent variables to fake data whose distribution is expected to closely match the real data distribution. *Generative adversarial networks* (GAN) [6] and *variational auto-encoders* (VAE) [14] are representative work in this category.

GANs build a two player game where the generator consecutively produces fake data to deceive the discriminator while the discriminator simultaneously improves its judgment, theoretically yielding a min-max problem. The objective of vanilla GANs, formed as a zero-sum game, amounts to minimization of the *Jensen-Shannon* (JS) divergence between the fake data distribution and the real data distributions. Recent advancements in development of GANs suggest three perspectives: (1) density ratio estimation [23, 29]; (2) kernel two-sample tests [18, 5, 27, 17, 2] and (3) optimal transport [1, 8, 21]. Density ratio estimation relies on evaluating a certain function of density ratio, generally not well-defined for distributions whose support are low-dimensional manifolds. Kernel two-sample tests and optimal transport commonly borrow strength from the classical *integral probability metrics* (IPM) [22, 26], giving birth to efficient and effective methods such as MMD GAN [18], [5] and Wasserstein GAN [1].

VAEs constrain the latent space with a simple prior and perform approximate maximum likelihood estimation via maximizing the corresponding evidence lower bound (ELBO). ELBO-based deep generative learning enjoys optimization stability but was disputed for generating blurry image samples. In fact, ELBO can be decomposed into a data space fitting term and a latent space regularization term, motivating a better design of the objective function by refining either the data fitting term or the regularization term. For example, Adversarial auto-encoders (AAE) [20] use GANs to better regularize the aggregated posterior of latent codes. Wasserstein auto-encoders (WAE) [28], from the viewpoint of optimal transport, generalize AAEs with *penalized optimal transport* (POT) objectives [3]. Similar ideas are found in some works on disentangled representations of natural images [12], [15].

In this work, we propose a novel generative model named *Wasserstein-Wasserstein auto-encoders* (WWAE), where the squared Wasserstein-2 distance is employed to match the aggregated posterior of latent codes with a Gaussian prior while the generative model is learned via minimizing a penalized optimal optimal transport.

1.2 Contributions

Our main contributions are as follows:

- We enrich the POT generative modeling framework by considering minimization of Wasserstein distances that are characterized for metrizing weak convergence of probability measures [32] in latent code space. WWAE naturally inherits the theoretical no-blurriness generation advantage of POT-based AEs [3].
- Instead of using a superfluous GAN involved in AAE or WAE-GAN [28], the proposed WWAE utilizes the closed-form Fréchet distance for two Gaussians [4]. As a result, WWAE does not suffer from the the sampling burden in WAE-MMD [28] and it is computationally efficient by leveraging the reparameterization trick in VAE.
- Empirically, WWAEs generate samples of higher visual quality than VAEs and WAEs when evaluated on multiple benchmark datasets, including MNIST, fashion-MNIST and CelebA. For FID scores [10], WWAE matches or outperforms VAEs and WAEs.

2 WWAE

2.1 Background, Notation

Let $\{\mathbf{X}_i\}_{i=1}^N \in \mathcal{X} \subset \mathcal{R}^d$ be independent and identically distributed samples from an unknown target distribution P_X living in the probability space $\mathcal{P}(\mathcal{X})$. We aim to learn a deep neural network G_θ with parameter θ that transforms low dimensional random Gaussian samples $Z \in \mathcal{Z} \subset \mathcal{R}^\ell$ into samples from P_X . Let P_G denote the distribution of $G_\theta(Z)$ and the Wasserstein distance $W_c(P_X||P_G)$ (optimal transport loss) [31] to measure the discrepancy between P_X and P_G . Recall the Kantorovich’s formulation of the Wasserstein distance [31]:

$$W_c(P_X||P_G) = \inf_{\gamma \in \mathcal{C}(X \sim P_X, Y \sim P_G)} \{\mathbf{E}_{(X,Y) \sim \gamma} [\|X - Y\|_c^c]\},$$

where $\mathcal{C}(X \sim P_X, Y \sim P_G)$ is the coupling set of all joint distributions of (X, Y) with marginals P_X and P_G respectively, and $\|X - Y\|_c$ with $c \geq 1$ denotes the c norm on \mathcal{R}^d . Under the mild condition [3], by parameterizing the coupling set, the Wasserstein distance $W_c(P_X||P_G)$ can be equivalently reformulated as follows:

$$W_c(P_X||P_G) = \inf_{Q: Q_Z = P_Z} \mathbf{E}_{P_X} \mathbf{E}_{Q(Z|X)} [\|X - G_\theta(Z)\|_c^c], \quad (2.1)$$

where P_Z denote the Gaussian distribution in the latent space \mathcal{Z} , and Q_Z is the aggregated posterior distribution of Z when $X \sim P_X$, $Z \sim Q(Z|X)$, i.e., $q_Z(z) = \int p_X(x)q(z|x)dx$ with $q_Z(z)$, $p_X(x)$, and $q(z|x)$ being the corresponding densities of Q_Z , P_X , and $Q(Z|X)$, respectively. The POT loss $\widetilde{W}_c(P_X||P_G)$ is the Lagrangian version of (2.1) to handle the constraint $Q_Z = P_Z$, i.e.,

$$\begin{aligned} & \widetilde{W}_c(P_X||P_G) \\ &= \inf_Q \mathbf{E}_{P_X} \mathbf{E}_{Q(Z|X)} [\|X - G_\theta(Z)\|_c^c] + \lambda \cdot \mathcal{D}(Q_Z||P_Z), \end{aligned} \tag{2.2}$$

where $\mathcal{D}(Q_Z||P_Z)$ is a metric on probability space $\mathcal{P}(\mathcal{Z})$, and $\lambda > 0$ is the regularization parameter.

2.2 WWAE model and algorithm

In this section, we propose a new deep generative model named *Wasserstein-Wasserstein auto-encoders* (WWAE) in the framework of POT, where $\mathcal{D}(Q_Z||P_Z)$ is chosen as the Wasserstein distance $W_2(Q_Z||P_Z)$. The reasons that we propose to use Wasserstein distance $W_2(Q_Z||P_Z)$ as a regularizer are as follows:

- The Wasserstein distance is a weak metric [32] that gives more regularity of the objective functions, yielding a more stable algorithm for training [1].
- In deep generative models, the prior P_Z is often chosen as Gaussian. We also notice that the aggregated posterior Q_Z can also be approximated as Gaussian. In the mini-batch training procedure, we first sample n samples $X_i, i = 1, \dots, n$ from P_X . By using the reparametric trick, the corresponding latent codes \tilde{Z}_i sampled from $Q(Z|X_i)$ are Gaussian. Hence, $q_Z(z) = \int p_X(x)q(z|x)dx \approx \sum_{i=1}^n q(z|X_i)/n \approx \sum_{i=1}^n \tilde{Z}_i/n$ corresponds to a summation of a small number of encoded latent Gaussian codes which are approximately independent. The Wasserstein distance between two Gaussians is the so called the Fréchet distance which has a closed-form representation using their means and covariance matrices [4] and can be estimated efficiently from samples.

Here we recall that

$$\begin{aligned} W_2(P||Q) &= \|\mu_P - \mu_Q\|_2^2 + \text{Trace}(\Sigma_P) + \text{Trace}(\Sigma_Q) \\ &\quad - 2\text{Trace}(\Sigma_P^{\frac{1}{2}}\Sigma_Q^{\frac{1}{2}}), \end{aligned}$$

where P and Q are Gaussian with means and covariance matrices (μ_P, Σ_P) and (μ_Q, Σ_Q) , respectively.

Based on the above considerations, we propose to optimize the following objective function to learn WWAE:

$$\min_{G_\theta, Q_\phi} \mathbf{E}_{P_X} \mathbf{E}_{Q_\phi(Z|X)} [\|X - G_\theta(Z)\|_2^2] + \lambda \cdot W_2(Q_Z || P_Z), \quad (2.3)$$

where we parameterize the encoded distribution $Q(Z|X)$ using another deep neural network Q_ϕ with parameter ϕ . We propose the following algorithm to train WWAE model (2.3).

- Specify regularization parameter λ and batch-size n . Initialize the parameters of the encoder Q_ϕ decoder and generator G_θ .
- Loop
 - Sample mini-batch X_i from P_X and sample Z_i from P_Z , $i = 1, \dots, n$. Compute sample mean $\hat{\mu}_Z$ and sample covariance matrix $\hat{\Sigma}_Z$ using Z_i s.
 - Sample mini-batch \tilde{Z}_i , from $Q_\phi(Z|X_i)$, $i = 1, \dots, n$. Compute sample mean $\hat{\mu}_{\tilde{Z}}$ and sample covariance matrix $\hat{\Sigma}_{\tilde{Z}}$ using \tilde{Z}_i s.
 - Update ϕ, θ via descending

$$\begin{aligned} & \frac{1}{n} \sum_{i=1}^n \|X_i - G_\theta(\tilde{Z}_i)\|_2^2 + \lambda [\|\hat{\mu}_Z - \hat{\mu}_{\tilde{Z}}\|_2^2 \\ & + \text{Trace}(\hat{\Sigma}_Z) + \text{Trace}(\hat{\Sigma}_{\tilde{Z}}) - 2\text{Trace}(\hat{\Sigma}_Z^{\frac{1}{2}} \hat{\Sigma}_{\tilde{Z}}^{\frac{1}{2}})] \end{aligned}$$

with Adam [13].

- End Loop

By using the reparametric trick the latent codes \tilde{Z}_i and the estimated $\hat{\mu}_{\tilde{Z}}$ and $\hat{\Sigma}_{\tilde{Z}}$ are all functions of the neural network parameter ϕ . Therefore, the minimization problem in the last step in our above algorithm can be done via calling the stochastic gradient gradient solver such as the Adam [13].

2.3 Related works and discussion

The blurriness of VAEs is caused by the combination of the Gaussian decoder and the regularization term in VAEs see Section 4.1 in [3] for detail argument. The Gaussian

decoder is induced by the reparametric trick, which can not be avoided. The regularization term in VAEs measures the discrepancy between the marginal encoded distribution and the prior distribution. To reduce the blurry of VAEs, much attention has been paid to find a better regularization term.

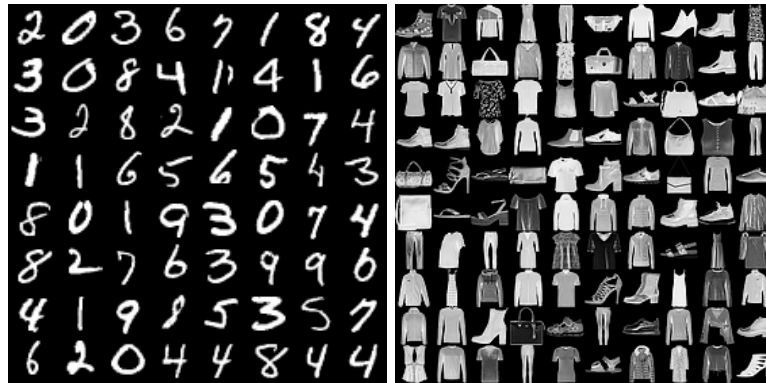
Along this line, some related works have been proposed in the framework of POT, aiming to improve the performance of deep generative models via refining the regularizer. Adversarial auto-encoders (AAE) [20] utilize GANs loss to regularize the aggregated posterior of latent codes. Wasserstein auto-encoders (WAE) [28], reformulated the AAEs into POT objectives [3], giving more insightful understanding of AAEs. [28], proposed using the maximum mean discrepancy (MMD) [7] between the aggregated posterior distribution and the prior latent distribution as the regularizer in (2). We enrich the POT generative modeling framework by considering the Wasserstein distances as a regularizer in the latent code space. The advantage of the proposed WWAE over superfluous GAN / MMD based regularizer in AAE or WAE-GAN [28] / WAE-MMD [28] is that the closed-form representation makes the computation more efficient and thus overcomes the sampling burden in WAE-MMD.

3 Experiment

In this section, we performed experiments to evaluate the proposed WWAE and compared its experimental results with some other closely related deep generative models. The experimental settings are presented in Section 3.1. The visualization-based quality illustration and the numerical quality analysis are shown in Section 3.2 and Section 3.3, respectively.

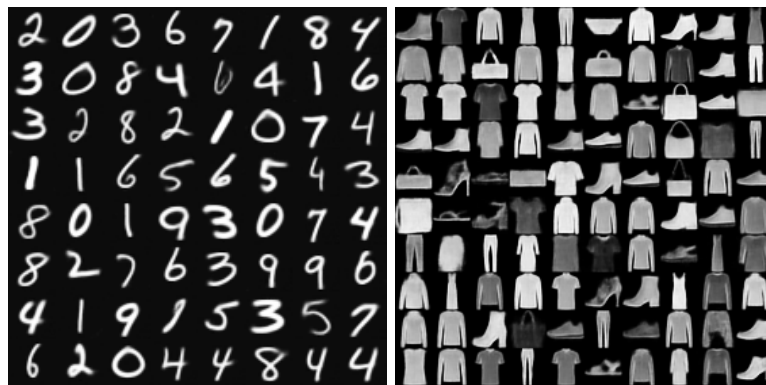
3.1 Experimental Settings

Dataset: We trained WWAE for image generation and reconstruction on the MNIST [16], Fashion-MNIST [33] and CelebA [19] datasets, where the size of training instances were 30K, 30K, 200K. For the CelebA dataset, we cropped and resized the image into 64×64 as the previous research.



(a) Real image

(b) Real image



(c) Reconstructed image

(d) Reconstructed image



(e) Generated image

(f) Generated image

Figure 1: Real samples, reconstructed samples and generated samples from WWAE with batch size 64 on the MNIST and Fashion-MNIST datasets.

Network architecture: In our experiments, we adopted the architecture of traditional convolution neural networks used in VAE to design decoder G_θ and encoder Q_ϕ . After a few experiments, however, we found that the traditional VAE architecture was too shallow to capture the high level features in images, as well as suffered from a slower rate of convergence. Therefore, we added several residual blocks [9] in both the encoder and the

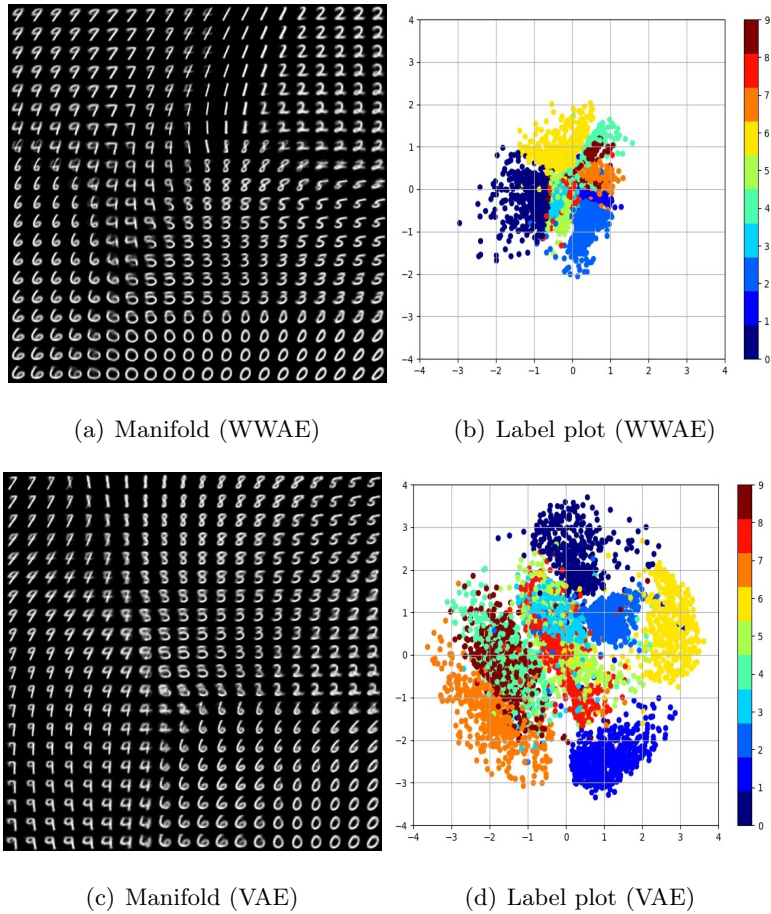


Figure 2: Manifolds learned by WWAE (a) and VAE (c) on MNIST, and distributions of latent codes learned by WWAE (b) and VAE (d) with labels.

decoder to extract more high-level features and improve the image quality. Specifically, we added two residual blocks between every two convolution layers in our encoder and decoder while maintained other network structure like DCGAN. **Hyper-parameters setting:** We used the Adam optimizer [13] with starting learning rate $r = 0.005$, $\beta_1 = 0.5$, $\beta_2 = 0.9$. We decayed our learning rate every 10K by 0.9 on MNIST, Fashion-MNIST and every 20K by 0.9 on CelebA dataset, respectively. We used batch normalization layers after each convolution layer except the final one, and used Relu activation function in our neural network. We choose batch size as 64 on MNIST and Fashion-MNIST, while increased batch size to 100 on CelebA.

3.2 Qualitative Analysis

Due to the relatively simple structure of images in MNIST and Fashion-MNIST, it is easier for WWAE to achieve a good performance on both reconstructed images and generated

images. As shown in Figure 1, images generated by WWAE not only have clear details but also achieved a fairly good diversity.

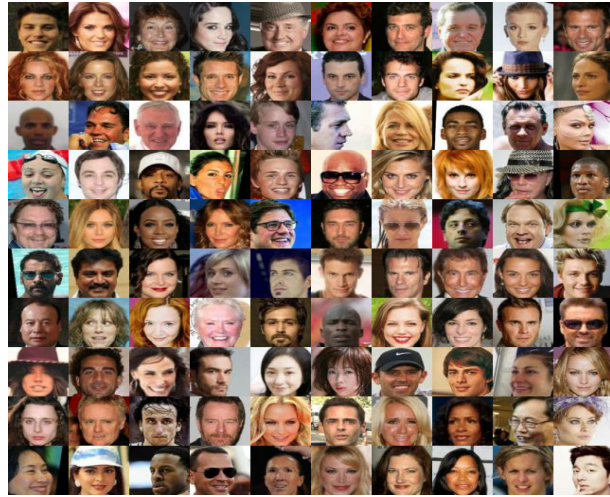
Figure 2 shows the learned manifolds based on the MNIST dataset when dimension of latent space equals to 2. Both VAE and our proposed WWAE can learn a manifold to represent the data structure. For the manifold learned by VAE, Figure 2 (d) shows that there are large holes between two different labels (e.g., digits 0 and 6). If an image whose latent code is collected from a hole, then the image can be blurry because its latent code would have to be averaged from its neighbors (e.g., the average of the latent codes of 0 and 6). This artifact has been greatly reduced for the manifold learned by WWAE shown in Figure 2 (b). The better performance of WWAE could be attributed to Wasserstein 2 distance as the regularizer. As a result, the generated image from WWAE can be less blurry than that from VAE. We also evaluated our model on a more complex RGB dataset CelebA. The results are shown in Figure 3. Furthermore, the latent space of WWAE on the CelebA dataset is visualized in Figure 4. We can see a smooth transform between two different faces, indicating a continuous and well-structured latent space representation has been learned by WWAE.

Model comparison: In order to demonstrate the sampling quality and convergence, we first compared our WWAE model with DCGAN which was one of most popular deep generative models in various applications and researches. Regarding the encoder-decoder framework, we made comparison between our WWAE model and VAE, WAE-MMD. In Figure 5, we show that WWAE can generative more realistic images without too much blur and distortion. However, the generated images from VAE are often blurry while the images generated from DCGAN and WAE-MMD are not quite stable, involving distortions and artifacts. We also observed the instability issue during the DCGAN training process, i.e., DCGAN often collapses if the training time is relatively long.

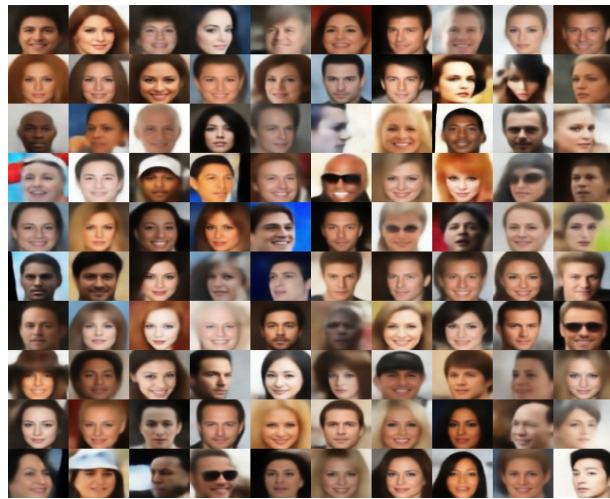
3.3 Quantitative Analysis

To quantitatively measure the quality and diversity of generated samples, we compute the Fréchet Inception Distance [11] score on CelebA dataset. The FID score is a numerical indicator which is more robust to noise than inception score and more sensitive to model collapse. It measures the quality of generated image samples by comparing the statistics of generated samples to real samples.

We first randomly selected 10k real images from the real datasets, serving as the



(a) Real image



(b) Reconstructed image



(c) Generated image

Figure 3: Real samples, reconstructed samples and generated samples from WWAE with batch size 100 on the CelebA dataset.

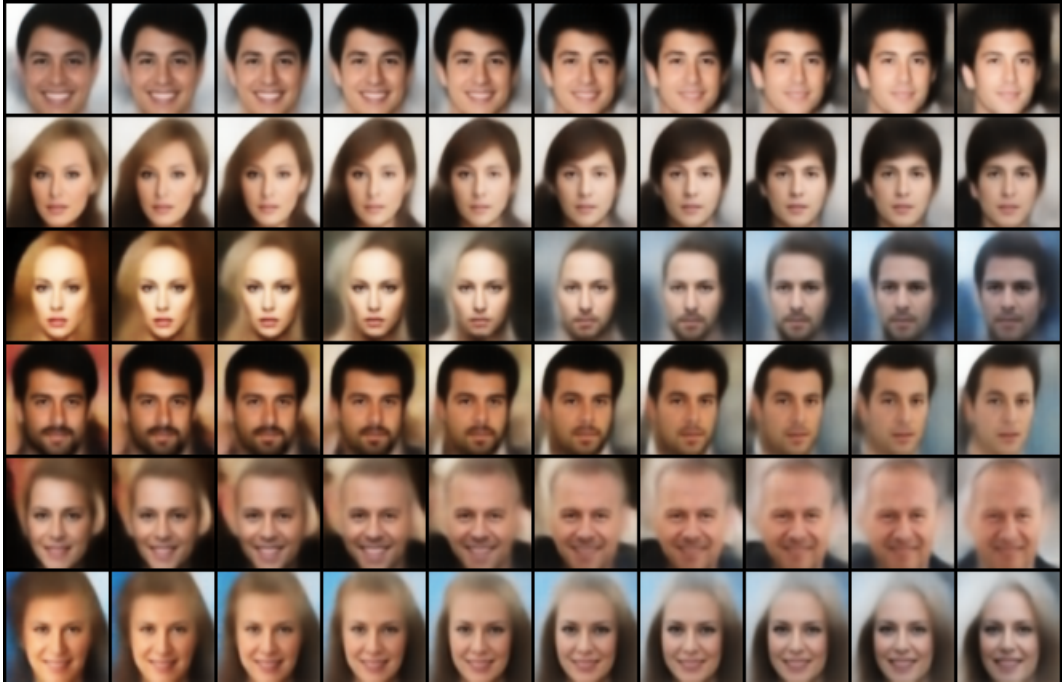


Figure 4: Latent space interpolation learned by WWAE.

Table 1: FID scores on MNIST, F-MNIST, and CelebA

Model	MNIST	F-MNIST	CelebA
Real data	1	1	2
WWAE	45	51	55
WAE-MMD	50	54	55
VAE	47	56	66
DCGAN	35	44	—

standard to compute the FID score. As shown in Table 1, we see that the proposed WWAE can achieve better FID score on all of the three datasets than WAE-MMD and VAE. Although DCGAN slightly outperformed WWAE on MNIST and Fashion MNIST, it failed to be stably applied to some more complex dataset, such as CelebA. To show a detailed comparison among WWAE, WAE-MMD, VAE and DCGAN, we calculated their FID scores every 5K iterations based on their generated 10K images. As shown in Figure 6, WWAE and WAE-MMD perform better than VAE, while DCGAN is confirmed to be unstable during the training process.

We note that WWAE and WAE-MMD have a very similar FID score on the CelebA dataset. Noticing that FID score is only a numerical criteria measuring the quality of



(a) WWAE

(b) VAE



(c) DCGAN

(d) WAE-MMD

Figure 5: Comparison between generated samples from WWAE, DCGAN, VAE and WAE-MMD.

generated images, it may not fully represent the visual quality by human eyes. In Figure 5, we show the generated images from the four different methods to compare their visual quality. Clearly, the quality of images generated by WWAE is better than that of the other methods.

4 Conclusion

In this paper, we propose a novel deep generative model named *Wasserstein-Wasserstein auto-encoders* (WWAE). We approximate the optimal transport loss of the target distribution and the generated distribution via penalized optimal transport where the squared Wasserstein-2 distance between the aggregated posterior of latent codes and a Gaussian

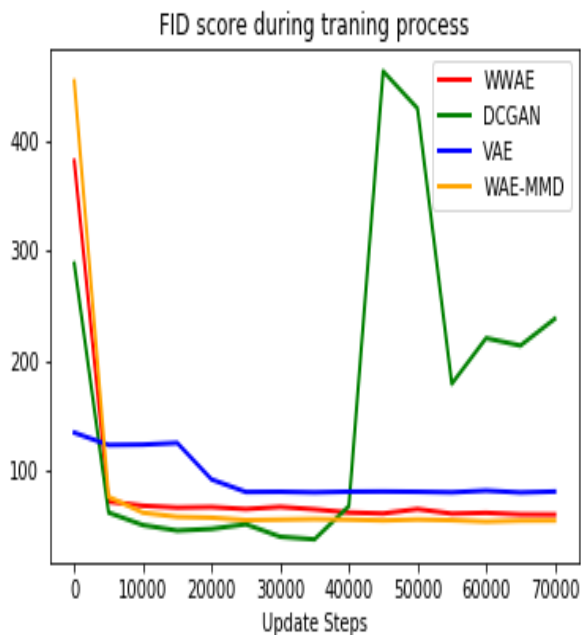


Figure 6: FID score comparison on celebA

prior is served as the penalty. WWAE reduces the blurriness of VAE and improve the stability of training deep generative models. Numerical results evaluated on multiple benchmark datasets including MNIST, fashion-MNIST and CelebA show that WWAE learns better latent structures than VAEs and generates samples of better visual quality and higher FID scores than VAEs and GANs. that WWAE learns better latent structures than VAEs and generates samples of better visual quality and higher FID scores than VAEs and GANs.

References

- [1] Martin Arjovsky, Soumith Chintala, and Léon Bottou. Wasserstein generative adversarial networks. In *International Conference on Machine Learning*, pages 214–223, 2017.
- [2] Mikołaj Bińkowski, Dougal J Sutherland, Michael Arbel, and Arthur Gretton. Demystifying MMD GANs. In *International Conference on Learning Representations*, 2018.
- [3] Olivier Bousquet, Sylvain Gelly, Ilya Tolstikhin, Carl-Johann Simon-Gabriel, and Bernhard Schoelkopf. From optimal transport to generative modeling: the vegan

cookbook. *arXiv preprint arXiv:1705.07642*, 2017.

- [4] DC Dowson and BV Landau. The fréchet distance between multivariate normal distributions. *Journal of multivariate analysis*, 12(3):450–455, 1982.
- [5] Gintare Karolina Dziugaite, Daniel M Roy, and Zoubin Ghahramani. Training generative neural networks via maximum mean discrepancy optimization. In *Proceedings of the Thirty-First Conference on Uncertainty in Artificial Intelligence*, pages 258–267. AUAI Press, 2015.
- [6] Ian Goodfellow, Jean Pouget-Abadie, Mehdi Mirza, Bing Xu, David Warde-Farley, Sherjil Ozair, Aaron Courville, and Yoshua Bengio. Generative adversarial nets. In *Advances in neural information processing systems*, pages 2672–2680, 2014.
- [7] Borgwardt-K. Rasch M. Schlkopf B. Gretton, A. and A. J. Smola. A kernel method for the two-sample-problem. In *Advances in Neural Information Processing Systems*, pages 513–520, 2007.
- [8] Ishaan Gulrajani, Faruk Ahmed, Martin Arjovsky, Vincent Dumoulin, and Aaron C Courville. Improved training of wasserstein gans. In *Advances in Neural Information Processing Systems*, pages 5767–5777, 2017.
- [9] Kaiming He, Xiangyu Zhang, Shaoqing Ren, and Jian Sun. Deep residual learning for image recognition. In *Proceedings of the IEEE conference on computer vision and pattern recognition*, pages 770–778, 2016.
- [10] Martin Heusel, Hubert Ramsauer, Thomas Unterthiner, Bernhard Nessler, and Sepp Hochreiter. Gans trained by a two time-scale update rule converge to a local nash equilibrium. In *Advances in Neural Information Processing Systems*, pages 6626–6637, 2017.
- [11] Martin Heusel, Hubert Ramsauer, Thomas Unterthiner, Bernhard Nessler, Günter Klambauer, and Sepp Hochreiter. Gans trained by a two time-scale update rule converge to a nash equilibrium. *arXiv preprint arXiv:1706.08500*, 12(1), 2017.
- [12] Irina Higgins, Loic Matthey, Arka Pal, Christopher Burgess, Xavier Glorot, Matthew Botvinick, Shakir Mohamed, and Alexander Lerchner. beta-vae: Learning basic visual concepts with a constrained variational framework. 2016.

- [13] Diederik P. Kingma and Jimmy Ba. Adam: A method for stochastic optimization. *arXiv preprint arXiv:1412.6980*, 2014.
- [14] Diederik P Kingma and Max Welling. Auto-encoding variational bayes. *arXiv preprint arXiv:1312.6114*, 2013.
- [15] Abhishek Kumar, Prasanna Sattigeri, and Avinash Balakrishnan. Variational inference of disentangled latent concepts from unlabeled observations. In *International Conference on Learning Representations*, 2018.
- [16] Yann LeCun, Corinna Cortes, and CJ Burges. Mnist handwritten digit database. *AT&T Labs [Online]*. Available: <http://yann.lecun.com/exdb/mnist>, 2, 2010.
- [17] Chun-Liang Li, Wei-Cheng Chang, Yu Cheng, Yiming Yang, and Barnabás Póczos. Mmd gan: Towards deeper understanding of moment matching network. In *Advances in Neural Information Processing Systems*, pages 2203–2213, 2017.
- [18] Yujia Li, Kevin Swersky, and Rich Zemel. Generative moment matching networks. In *International Conference on Machine Learning*, pages 1718–1727, 2015.
- [19] Ziwei Liu, Ping Luo, Xiaogang Wang, and Xiaoou Tang. Deep learning face attributes in the wild. In *Proceedings of International Conference on Computer Vision (ICCV)*, 2015.
- [20] Alireza Makhzani, Jonathon Shlens, Navdeep Jaitly, Ian Goodfellow, and Brendan Frey. Adversarial autoencoders. *arXiv preprint arXiv:1511.05644*, 2015.
- [21] Takeru Miyato, Toshiki Kataoka, Masanori Koyama, and Yuichi Yoshida. Spectral normalization for generative adversarial networks. In *International Conference on Learning Representations*, 2018.
- [22] Alfred Müller. Integral probability metrics and their generating classes of functions. *Advances in Applied Probability*, 29(2):429–443, 1997.
- [23] Sebastian Nowozin, Botond Cseke, and Ryota Tomioka. f-gan: Training generative neural samplers using variational divergence minimization. In *Advances in Neural Information Processing Systems*, pages 271–279, 2016.
- [24] Santiago Pascual, Antonio Bonafonte, and Joan Serra. Segan: Speech enhancement generative adversarial network. *Proc. Interspeech 2017*, pages 3642–3646, 2017.

- [25] Scott Reed, Zeynep Akata, Xinchun Yan, Lajanugen Logeswaran, Bernt Schiele, and Honglak Lee. Generative adversarial text to image synthesis. *arXiv preprint arXiv:1605.05396*, 2016.
- [26] Bharath K Sriperumbudur, Kenji Fukumizu, Arthur Gretton, Bernhard Schölkopf, Gert RG Lanckriet, et al. On the empirical estimation of integral probability metrics. *Electronic Journal of Statistics*, 6:1550–1599, 2012.
- [27] Dougal J Sutherland, Hsiao-Yu Tung, Heiko Strathmann, Soumyajit De, Aaditya Ramdas, Alex Smola, and Arthur Gretton. Generative models and model criticism via optimized maximum mean discrepancy. *arXiv preprint arXiv:1611.04488*, 2016.
- [28] Ilya Tolstikhin, Olivier Bousquet, Sylvain Gelly, and Bernhard Schoelkopf. Wasserstein auto-encoders. In *International Conference on Learning Representations*, 2018.
- [29] Masatoshi Uehara, Issei Sato, Masahiro Suzuki, Kotaro Nakayama, and Yutaka Matsuo. Generative adversarial nets from a density ratio estimation perspective. *arXiv preprint arXiv:1610.02920*, 2016.
- [30] Aäron Van Den Oord, Sander Dieleman, Heiga Zen, Karen Simonyan, Oriol Vinyals, Alex Graves, Nal Kalchbrenner, Andrew W Senior, and Koray Kavukcuoglu. Wavenet: A generative model for raw audio. In *SSW*, page 125, 2016.
- [31] Cédric Villani. *Optimal transport: old and new*, volume 338. Springer Science & Business Media, 2008.
- [32] Jonathan Weed and Francis Bach. Sharp asymptotic and finite-sample rates of convergence of empirical measures in wasserstein distance. *arXiv preprint arXiv:1707.00087*, 2017.
- [33] Han Xiao, Kashif Rasul, and Roland Vollgraf. Fashion-mnist: a novel image dataset for benchmarking machine learning algorithms. *arXiv preprint arXiv:1708.07747*, 2017.
- [34] Jun-Yan Zhu, Taesung Park, Phillip Isola, and Alexei A Efros. Unpaired image-to-image translation using cycle-consistent adversarial networks. *IEEE International Conference on Computer Vision*, Oct 2017.